Measurements of the Higgs Boson Properties at the ATLAS Experiment

Elisabeth Schopf, on behalf of the ATLAS Collaboration

After the discovery of the Higgs boson in summer 2012, the understanding of its properties has been a high priority of the physics program of the ATLAS experiment. Measurements of Higgs boson properties sensitive to its production processes, decay modes, kinematics and mass based on LHC proton-proton collision data recorded at 13 TeV are presented. Analyses in several decay channels and the combination of different measurements are discussed.

1 Introduction

The Standard Model (SM) of elementary particles describes the known fundamental particles and their interactions. It includes three generations of quark and lepton pairs each. In addition, five bosons are included in the SM: the photon, which is the force carrier of the electromagnetic force, the $W^\pm$ and Z boson, which are the force carriers of the weak force, the gluon, which is the force carrier of the strong force, and the Higgs boson which is associated to the Higgs mechanism. The Higgs mechanism was proposed to give mass to the $W^\pm$ and Z boson after it was discovered experimentally that they have a substantial mass [1, 2]. The Higgs mechanism introduces an additional field, the Higgs field, which is present everywhere in the universe and particles gain their masses by interactions with it. This means that the coupling strength of a given particle to the Higgs field is directly proportional to the particle's mass. In contrast to interactions of $W^\pm$ and Z boson with the Higgs field, which arise from the Higgs mechanism by construction, interactions of fermions were added ad-hoc to generate their masses via interactions with the Higgs field as well. Therefore there is a fundamental difference between fermionic interactions and $W^\pm$ and Z boson interactions that make it important to experimentally observe both types of couplings.

Excitations of the Higgs field manifest as an observable scalar boson: the Higgs boson. The mass of the Higgs boson is a free parameter whereas the charge (0) and spin (0) are predicted by theory. Extensive searches for the Higgs boson probing various mass ranges were conducted over the years leading to the discovery in 2012 of a boson with properties consistent with those of the SM Higgs boson by the ATLAS [3] and CMS experiment [4]. The mass of this boson was determined to be approximately 125 GeV. This discovery was obtained using LHC proton-proton collisions of the so-called run 1, which is the run period from 2010 to 2012 during which the LHC operated at a collision energy of 7 TeV and 8 TeV. Since its discovery the properties of the Higgs boson are continuously studied. The latest results are obtained with the run 2 data of the LHC which are being recorded since 2015 at a collision energy of 13 TeV. A short description of the ATLAS detector is given in section 2 and details about the Higgs boson production and decay channels are given in section 3. Highlights of the results by the ATLAS experiment are presented in sections 4 and 5 while the latest combination of Higgs boson measurements is shown in section 6.

2 The ATLAS detector

The ATLAS detector [5] at the LHC covers nearly the entire solid angle around the collision point. It consists of an inner tracking detector surrounded by a thin superconducting solenoid, electromagnetic and hadronic calorimeters, and a muon spectrometer incorporating three large superconducting toroidal magnets. The inner-detector system (ID) is immersed in a 2 T axial magnetic field and provides charged particle tracking in the range $|\eta| < 2.5$.

The inner detector consists of a high-granularity silicon pixel detector, surrounded by the silicon microstrip tracker which is enclosed by the transition radiation tracker. These systems reconstruct the tracks of charged particles and provide a momentum measurement since they are immersed in a magnetic field.

The calorimeter system consists of an electromagnetic calorimeter, which is followed by a hadronic calorimeter. The former providing energy measurements of photons and electrons and the latter providing energy measurements of hadrons.

The muon spectrometer (MS) measures the deflection of muons in a magnetic field generated by superconducting air-core toroids. It provides additional tracking and momentum information for muons.

3 Higgs boson production and decay

The production cross section for the Higgs boson in various production channels can be predicted once the Higgs boson mass and the proton-proton collision energy are known. The predictions presented in the following assume a proton-proton collision energy of 13 TeV and a Higgs boson mass of 125 GeV. In general, approximately only one in one billion proton-proton collisions at the LHC produce a Higgs boson. The most likely production process is so-called gluon-gluon fusion (ggF), which produces a Higgs boson via a gluon induced loop of heavy particles. This production channel has a cross section of 48.6 pb. The second largest production channel is vector boson fusion (VBF) with a production cross section of 3.8 pb. In the VBF mode two W or Z bosons, radiated off the quarks in the protons, fuse together to form a Higgs boson. The characteristic signature of this production channel are two quarks that are produced in association with the Higgs boson and which are typically emitted in the forward directions of the detector. In the so-called VH production channel, the Higgs boson is produced by being radiated off a W or Z boson. This means the final state contains a W or Z boson in addition to the Higgs boson. The production cross sections are 1.4 pb for WH and 0.9 pb for ZH production. Another production channel probed by the ATLAS experiment is so-called ttH production, where the Higgs boson is produced in association with a top-quark pair. This production channel has a production cross section of 0.5 pb. All values are taken from [6].

Since the Higgs boson is unstable it immediately decays after its production. Figure 1 shows a pie chart of the predicted Higgs boson branching ratios into the SM particles, assuming a Higgs boson mass of 125 GeV. The most probable decay is the decay into a pair of bottom quarks with a BR of 58%. The decay into a pair of WW bosons has the second largest BR of 21%. Decays into other bosons or lighter fermions have decay rates below 10%. All values are taken from [6].
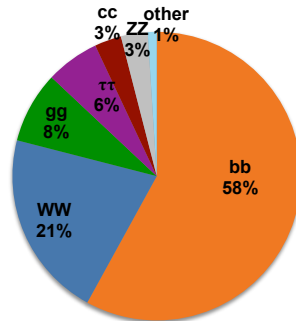

Figure 1: Branching ratios for the SM Higgs boson with a mass of 125 GeV.

4 $H \rightarrow ZZ$ and $H \rightarrow \gamma\gamma$ measurements

Decays of the Higgs boson into a pair of photons or Z bosons have very low branching ratios of 0.2% and 3% respectively, but excellent mass resolution. Both channels have final state particles (photons or electron, muons from $Z \rightarrow ee$, $\mu\mu$ decays) that can be measured with a good experimental resolution and have only one major, well modelled background source ($\gamma\gamma$ continuum and ZZ production) each. $H \rightarrow \gamma\gamma$ candidate events are identified by requiring two isolated well separated photons. $H \rightarrow ZZ$ measurements

target events, where the Z bosons decays into electrons or muons. Therefore the experimental signature is either 4 electrons, 4 muons or 2 electrons and 2 muons. This signature is referred to as 4 leptons in the following. In addition, the total electrical charge of the electrons and muons has to be 0.

4.1 Higgs boson mass and width

The Higgs boson mass is extracted from the invariant mass of the photon pair or the 4 leptons and is measured to be 124.93 ± 0.40 GeV and 124.79 ± 0.37 GeV respectively [7]. Both measurements are well compatible with each other and were obtained using 36.1 fb^{-1} of LHC data at a collision energy of 13 TeV. Figure 2 shows the invariant mass spectrums in both analysis channels. The combination of those two run 2 measurements and the run 1 measurement determines the Higgs boson mass m_H to be [7]:

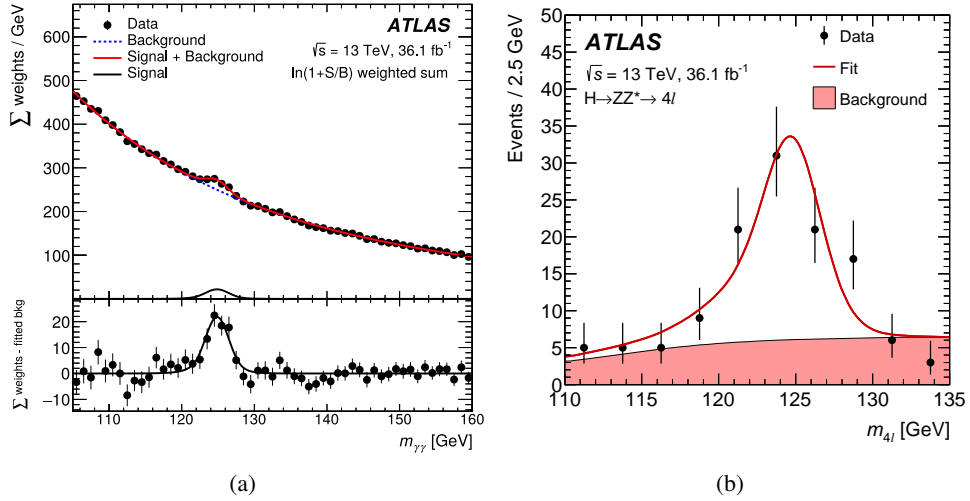$$m_H = (124.97 \pm 0.24) \text{ GeV} \tag{1}$$

Figure 2: The invariant di-photon mass (a) and 4 lepton mass (b) from the $H \rightarrow \gamma\gamma$ and $H \rightarrow ZZ$ analysis channels [7].

These analyses can also be used to set a limit on the total decay width of the Higgs boson from the line shape of the invariant mass peak. However, due to the experimental mass resolution, this limit is more than 1000 times higher than the predicted SM total decay width Γ_H^{SM} of approximately 4 MeV assuming a Higgs boson mass of 125 GeV and only SM decays [6]. Another indirect way to constrain the total decay width of the Higgs boson is to set a limit on unobserved Higgs boson decays that could contribute to the total width. The combination of measurements from various Higgs boson decay channels – including decays into fermions – using 13 TeV data yields an upper limit at the 95% confidence level (CL) of BR($H \rightarrow$ unobserved) = 0.26 [8]. The currently most stringent, indirect limit on the total Higgs boson decay width is obtained from a measurement of the ratio of on-shell to off-shell Higgs boson production in the $H \rightarrow ZZ$ decay channel. This analysis probes the 4 lepton channel and additionally the $H \rightarrow Z(ee, \mu\mu)Z(\nu\nu)$ channel to increase data statistics. An upper 95% CL limit on Γ_H^{SM} is set at 14.4 MeV [9].

4.2 Differential measurements

Increasing data statistics make it possible to perform differential measurements for the Higgs boson in the $H \rightarrow \gamma\gamma$ and $H \rightarrow ZZ$ decay channels. Differential measurements are sensible to unexpected Higgs interactions that might be hidden in measurements of the total Higgs boson cross sections. Therefore these measurements offer a window to probe new physics. Figure 3 shows the measurement of the transverse momentum of the Higgs boson in the di-photon and 4 lepton decay channels using 79.8 fb^{-1} of 13 TeV data. The measurements are compared to several theoretical predictions, which are compatible with the data within the uncertainties. The analyses described in [10] and [11] also provide a differential measurement for the number of jets in the final state. In addition, the di-photon analysis probes the distribution of the Higgs boson rapidity. In all cases no significant deviations from the theoretical expectations are observed.
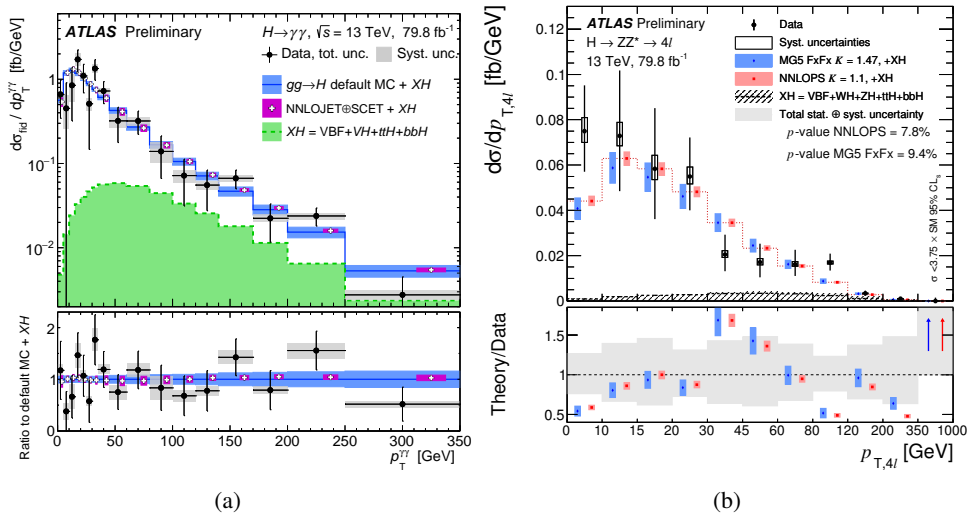

Figure 3: The distribution of the Higgs boson transverse momentum in the di-photon [10] (a) and 4 lepton [11] (b) decay channels. The data (black points) is compared to several theoretical predictions.

5 Higgs-fermion coupling measurements

Due to the fundamental difference of Higgs-fermion couplings from Higgs-W/Z couplings, as described in section 1, it is essential to observe those couplings to gain confidence in the fermion mass generation mechanism. However, during run 1 of the LHC that successfully observed Higgs boson couplings to W and Z bosons the only coupling to fermions that was observed was the coupling to τ-leptons. Therefore establishing Higgs-fermion couplings also in other fermion channels is one of the goals for run 2 of the LHC.

5.1 $H \rightarrow b\bar{b}$ decays

The decay of the Higgs boson to a pair of bottom quarks is the decay channel with the highest probability (58%) but it is experimentally challenging. The experimental challenges are the identification of b-jets and

the high amount of background processes with hadronic signatures. Three separate analyses that target different Higgs boson production processes probe the $H \rightarrow b\bar{b}$ decay: VH, VBF and ttH. In all three cases b-jet are identified using a multivariate algorithm that discriminates b-jets from non-b-jets. The multivariate algorithm exploits the difference in lifetime between b-hadrons and lighter hadrons and combines this and other jet information, e.g. kinematics. The long lifetime of b-hadrons allows to resolve secondary decay vertices and produces charged particles, whose tracks have a significant impact parameter. More details on b-jet identification is given in [12, 13]. The VH analysis provides by far the best sensitivity for $H \rightarrow b\bar{b}$ decays since the decay of the W or Z boson to leptons suppresses a significant amount of multi-jet background and provides a good trigger signature. The $VH(b\bar{b})$ analysis probes three different vector boson decays: $Z \rightarrow \nu\nu$, $W \rightarrow (e, \mu)\nu$ and $Z \rightarrow ee, \mu\mu$. Signal candidate events are identified by requiring two b-jets and either a significant amount of missing transverse energy caused by the neutrinos, exactly one electron or muon plus missing transverse energy or exactly two electrons or two muons. To further enhance the sensitivity of this analysis a multivariate algorithm that separates signal from background events is used as the final discriminant of the analysis. The VH analysis yields an observed (expected) significance of $4.9(4.3)\sigma$ using 79.8 fb^{-1} of 13 TeV data [14]. The combination of this measurement with the measurement in the VBF and ttH analyses also taking into account the results from run 1 yields an observed (expected) significance of $5.4(5.5)\sigma$ and the signal strength $\mu = N_{\text{signal}}^{\text{measured}}/N_{\text{signal}}^{\text{expected}}$ is measured to be:

$$\mu = 1.01 \pm 0.12(\text{stat.})_{-0.15}^{+0.16}(\text{syst.}) \tag{2}$$

Therefore an observation of $H \rightarrow b\bar{b}$ decays is obtained and the measurement is compatible with the SM expectation [14]. More details on the VBF and ttH analyses are given in [15] and [16] respectively.

In addition, the $VH(b\bar{b})$ measurement is combined with the $VH(\gamma\gamma)$ and $VH(ZZ)$ measurements yielding an observed (expected) significance of $5.3(4.8)\sigma$, which corresponds to an observation of VH production. The measured VH signal strength is $1.13 \pm 0.15(\text{stat.})_{-0.17}^{+0.18}(\text{syst.})$ [14].

Figure 4 summarises the measured signal strengths of the individual $H \rightarrow b\bar{b}$ and VH analyses as well as their combination. In all cases the measurement is compatible with the SM expectation.
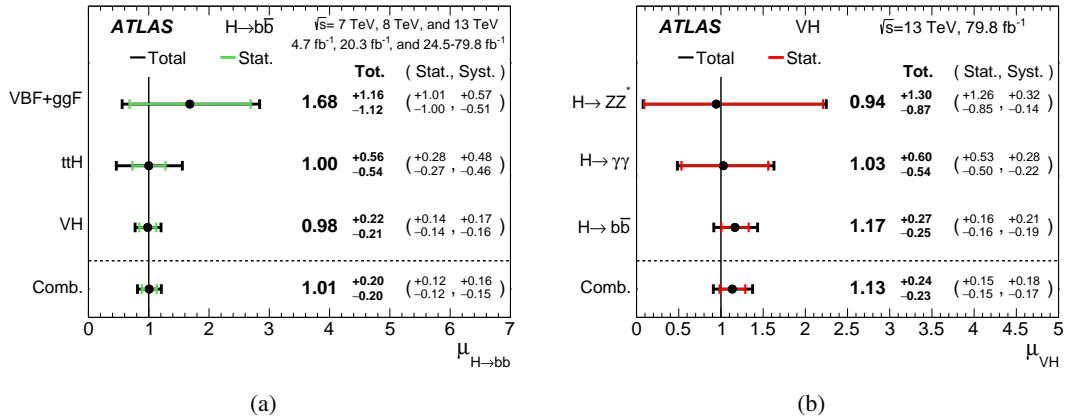

Figure 4: The measured signal strengths of the analyses targeting $H \rightarrow b\bar{b}$ decays (a) and VH production (b) [14].

6

5.2 ttH production

The coupling of the Higgs boson to the heaviest known SM particle, the top quark, can only be probed directly in the ttH production channel. However, most knowledge about this coupling that was obtained during run 1 was only indirect and originated from the ggF process assuming that top quarks are the main contributor to the loop. In run 2 the ttH production cross section is increased approximately by a factor of four due to the increase in collision energy. Nevertheless, the measurement of this process remains experimentally challenging due to the complex final states that arise from the decays of the two top quarks in addition to the signature from the Higgs boson decay. Four separate analyses target ttH production: $ttH(\gamma\gamma)$, $ttH(ZZ)$, $ttH(b\bar{b})$ and $ttH \rightarrow$ multi-lepton final states. The main contributors to the latter are $H \rightarrow WW$, $H \rightarrow \tau\tau$ and $H \rightarrow ZZ$ decays. All four analyses make use of machine learning algorithms and introduce several analysis categories that probe different combinations of possible top quark and Higgs boson decays to enhance the sensitivity to ttH events. The analyses with the largest sensitivity are the $ttH(\gamma\gamma)$ and ttH multi-lepton analysis. Their respective observed (expected) significances are $4.1(3.7)\sigma$ using 79.8 fb^{-1} of 13 TeV data [17] and $4.1(2.8)\sigma$ using 36.1 fb^{-1} of 13 TeV data [18]. The combination of all ttH measurements also taking into account the respective run 1 analyses, yields an observation with an observed (expected) significance of $6.3(5.1)\sigma$ and the measured signal strength μ is [17]:

$$\mu = 1.32 \pm 0.18(\text{stat.})^{+0.21}_{-0.19}(\text{syst.}) \tag{3}$$

Figure 5 shows the measured signal strengths in the ttH analyses as well as their combination, which are all compatible with the SM expectation within 2σ.
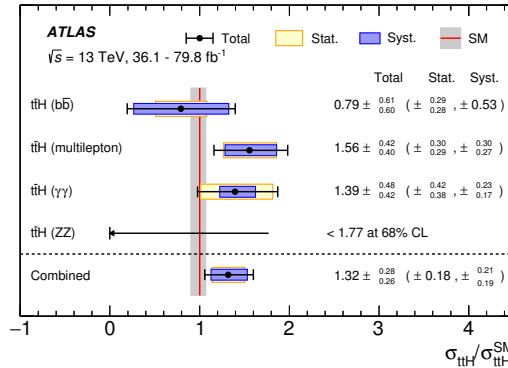

Figure 5: The measured signal strengths of the analyses targeting ttH production [17].

5.3 Higgs boson decays to light fermions

The decay of Higgs bosons to light fermions have small BRs due to the dependence of the coupling strength and the fermion mass. In run 2 two tree level decays are probed with the ATLAS experiment: Higgs boson decays to a pair of charm quarks (BR= 3%) and decays to a pair of muons (BR= 0.02%).

The $H \rightarrow c\bar{c}$ analysis uses specific c-jet identification algorithms, which were optimised for this analysis. To enhance the ratio of expected signal to background events the analysis targets $Z(ee, \mu\mu)H(c\bar{c})$ events. The measured upper limit on the signal strength μ with respect to the SM expectation is $\mu < 110$ at the 95% confidence level [19].

The $H \rightarrow \mu\mu$ analysis targets ggF and VBF production and makes use of a multivariate classifier to define analysis categories to enhance the sensitivity. The measured upper limit on the signal strength μ with respect to the SM expectation is $\mu < 2.1$ at the 95% confidence level [20].

6 Combination of Higgs boson measurements

The combination of the ATLAS Higgs boson measurements using up to 79.8 fb^{-1} of 13 TeV data includes the Higgs boson decays to $\gamma\gamma$, ZZ, WW, $\tau\tau$, $b\bar{b}$ and $\mu\mu$ and the ggF, VBF, VH and ttH production processes. The measured signal strength with respect to the SM expectation is [8]:

$$\mu = 1.13^{+0.09}_{-0.08} \tag{4}$$

Figure 6(a) shows the measured signal strengths in the Higgs boson production and decay channels probed by the ATLAS experiment using LHC run 2 data. No significant deviations from the SM expectation are observed. The measurements can also be interpreted as measurements of the corresponding coupling modifiers. Figure 6(b) shows the measured coupling strengths modifiers as a function of the mass of the particle the Higgs boson couples to. All measurements are compatible with the SM expectation that the coupling strengths modifiers scale linearly with the particle mass.
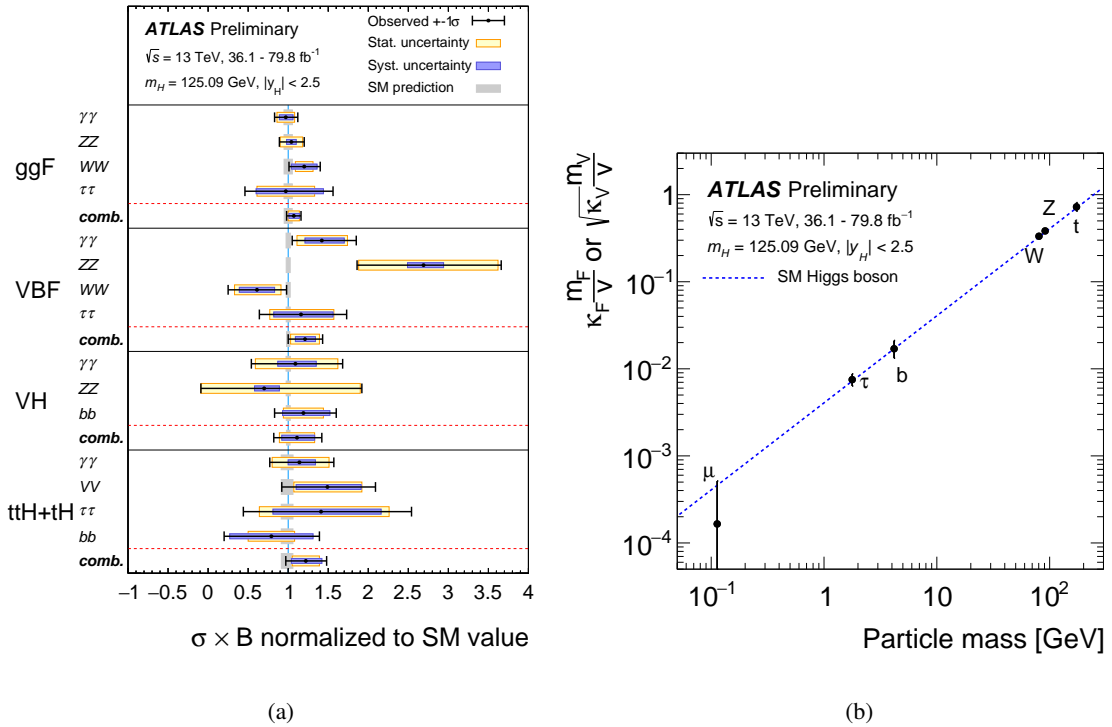

(a)　　　　　　　　　　　　　　　(b)

Figure 6: The measured Higgs boson signal strengths split into production processes and Higgs boson decay channels as well as their combination (a) [8]. The measured Higgs boson coupling strength modifiers as a function of the mass of the particles (b) [8].

7 Conclusion

The latest Higgs boson measurements of the ATLAS experiment are presented and no significant deviations from the SM expectation are observed. The results are obtained using up to 79.8 fb^{-1} of LHC proton-proton collisions at a collision energy of 13 TeV. The Higgs boson is now observed in five different decay modes ($\gamma\gamma$, ZZ, WW, $\tau\tau$, $b\bar{b}$) and four different production modes (ggF, VBF, VH, ttH). The mass of the Higgs boson is measured to be 124.97 ± 0.24 GeV and the best, but indirect, constraint on the Higgs boson total width is $\Gamma_H^{\text{SM}} < 14.4$ MeV. In addition to the recently achieved observations of the $b\bar{b}$ decay, VH production and ttH production, the ATLAS experiment also performed differential measurements in the $H \rightarrow \gamma\gamma$ and $H \rightarrow ZZ$ analysis channels. Precision measurements of the Higgs boson will continue with the larger data set that will be delivered by the LHC.

References

[1] F. Englert and R. Brout, *Broken Symmetry and the Mass of Gauge Vector Mesons*, Phys. Rev. Lett. **13** (9 1964) 321, URL: https://link.aps.org/doi/10.1103/PhysRevLett.13.321.

[2] P. W. Higgs, *Broken Symmetries and the Masses of Gauge Bosons*, Phys. Rev. Lett. **13** (16 1964) 508, URL: https://link.aps.org/doi/10.1103/PhysRevLett.13.508.

[3] ATLAS Collaboration, *A Particle Consistent with the Higgs Boson Observed with the ATLAS Detector at the Large Hadron Collider*, Science **338** (2012) 1576.

[4] CMS Collaboration, *Observation of a new boson at a mass of 125 GeV with the CMS experiment at the LHC*, Phys. Lett. B **716** (2012) 30, arXiv: 1207.7235 [hep-ex].

[5] ATLAS Collaboration, *The ATLAS Experiment at the CERN Large Hadron Collider*, JINST **3** (2008) S08003.

[6] D. de Florian et al., *Handbook of LHC Higgs Cross Sections: 4. Deciphering the Nature of the Higgs Sector*, (2016), arXiv: 1610.07922 [hep-ph].

[7] ATLAS Collaboration, *Measurement of the Higgs boson mass in the $H \rightarrow ZZ^* \rightarrow 4\ell$ and $H \rightarrow \gamma\gamma$ channels with $\sqrt{s} = 13$ TeV pp collisions using the ATLAS detector*, Phys. Lett. B **784** (2018) 345, arXiv: 1806.00242 [hep-ex].

[8] ATLAS Collaboration, *Combined measurements of Higgs boson production and decay using up to 80 fb^{-1} of proton–proton collision data at $\sqrt{s} = 13$ TeV collected with the ATLAS experiment*, ATLAS-CONF-2018-031, 2018, URL: https://cds.cern.ch/record/2629412.

[9] ATLAS Collaboration, *Constraints on off-shell Higgs boson production and the Higgs boson total width in $ZZ \rightarrow 4\ell$ and $ZZ \rightarrow 2\ell 2\nu$ final states with the ATLAS detector*, Phys. Lett. B **786** (2018) 223, arXiv: 1808.01191 [hep-ex].

[10] ATLAS Collaboration, *Measurement of Higgs boson properties in the diphoton decay channel using 80 fb^{-1} of pp collision data at $\sqrt{s} = 13$ TeV with the ATLAS detector*, ATLAS-CONF-2018-028, 2018, URL: https://cds.cern.ch/record/2628771.

[11] ATLAS Collaboration, *Measurements of the Higgs boson production, fiducial and differential cross sections in the 4ℓ decay channel at $\sqrt{s}$ = 13 TeV with the ATLAS detector*, ATLAS-CONF-2018-018, 2018, URL: https://cds.cern.ch/record/2621479.

[12] ATLAS Collaboration, *Performance of b-jet identification in the ATLAS experiment*, JINST **11** (2016) P04008, arXiv: 1512.01094 [hep-ex].

[13] ATLAS Collaboration, *Optimisation and performance studies of the ATLAS b-tagging algorithms for the 2017-18 LHC run*, ATL-PHYS-PUB-2017-013, 2017, URL: https://cds.cern.ch/record/2273281.

[14] ATLAS Collaboration, *Observation of $H \to b\bar{b}$ decays and VH production with the ATLAS detector*, Phys. Lett. B **786** (2018) 59, arXiv: 1808.08238 [hep-ex].

[15] ATLAS Collaboration, *Search for Higgs bosons produced via vector-boson fusion and decaying into bottom quark pairs in $\sqrt{s}$ = 13 TeV pp collisions with the ATLAS detector*, Phys. Rev. D **98** (2018) 052003, arXiv: 1807.08639 [hep-ex].

[16] ATLAS Collaboration, *Search for the standard model Higgs boson produced in association with top quarks and decaying into a $b\bar{b}$ pair in pp collisions at $\sqrt{s}$ = 13 TeV with the ATLAS detector*, Phys. Rev. D **97** (2018) 072016, arXiv: 1712.08895 [hep-ex].

[17] ATLAS Collaboration, *Observation of Higgs boson production in association with a top quark pair at the LHC with the ATLAS detector*, Phys. Lett. B **784** (2018) 173, arXiv: 1806.00425 [hep-ex].

[18] ATLAS Collaboration, *Evidence for the associated production of the Higgs boson and a top quark pair with the ATLAS detector*, Phys. Rev. D **97** (2018) 072003, arXiv: 1712.08891 [hep-ex].

[19] ATLAS Collaboration, *Search for the Decay of the Higgs Boson to Charm Quarks with the ATLAS Experiment*, Phys. Rev. Lett. **120** (2018) 211802, arXiv: 1802.04329 [hep-ex].

[20] ATLAS Collaboration, *A search for the rare decay of the Standard Model Higgs boson to dimuons in pp collisions at $\sqrt{s}$ = 13 TeV with the ATLAS detector*, ATLAS-CONF-2018-026, 2018, URL: https://cds.cern.ch/record/2628763.